High-Performance Polyimide-Based ReRAM for Nonvolatile Memory Application

Sheng-Hsien Liu, Wen-Luh Yang, Chi-Chang Wu, Tien-Sheng Chao, Meng-Ru Ye, Yu-Yuan Su, Po-Yang Wang, and Ming-Jui Tsai

***Abstract*—In this letter, high-performance polyimide (PI)-based resistive random access memory (ReRAM) is presented by utilizing a new DAXIN-PI thin film as a resistance layer. The switching between high- and low-resistance states is triggered by the formation and dissociation of the charge transfer complex. As compared with the electrochemical-metallization-based ReRAM and the valence-change-based ReRAM, this DAXIN-PI ReRAM shows excellent performance, including large Ron/Roff ratio, superior endurance, low operation voltage, fast switching speed, needless of a forming process, and acceptable retention characteristics. Among them, large Ron/Roff ratio ($> 10^5$) and superior endurance ($> 10^5$ cycles) can be simultaneously achieved, and the detailed reliability test for PI-based ReRAMs has been analyzed for the first time.**

***Index Terms*—Polyimide (PI), resistive random access memory (ReRAM) devices, sol–gel.**

I. Introduction

RECENTLY, resistive random access memory (ReRAM) devices have been widely studied to be a promising candidate of the next-generation nonvolatile memory due to high-shrinking capability and simple structure [1]. Typical ReRAMs have been divided into two main types, namely, electrochemical metallization memory (ECM) and valence change memory (VCM). The ECM relies on an electrochemically active electrode metal such as Cu [2]. Its on/off switching is controlled by the formation and dissociation of metallic filament. On the other hand, specific transition metal oxides such as HfO_x [3] have been used as a resistance layer of the VCM. Its on/off transformation is triggered by the migration of oxygen anions. In general, as compared with the ECM, the VCM has better reliability properties, particularly for endurance. On the contrary, the ECM generally has a wider memory window. As can be easily seen, large-capacity and high-reliability properties are difficult to be simultaneously obtained for ReRAMs.

In this letter, a new polyimide (DAXIN-PI) thin film is proposed as a resistance layer for ReRAM applications. Through this DAXIN-PI ReRAM, large Ron/Roff ratio and superior endurance properties can be easily and synchronously achieved. In addition, the detailed reliability properties of polymer-based ReRAMs have been completely studied for the first time [4]–[13].

II. Experiments

The sample, in a metal–organic–metal structure, was prepared on a glass substrate. The polymer acid (PAA) was prepared from 4-diaminodiphenylmethane (MDA) and 1, 2, 3, 4-cyclobutane tetracarboxylic dianhydride (CBDA). MDA (9.913 g, 0.05 mol) was dissolved in N-methyl-2-pyrrolidone (NMP) (89.4 g) under N_2 atmosphere. After 10 min, CBDA (CAS: 4415-87-6, 9.805 g, 0.05 mol) and NMP (22.3 g) were added into the reaction solution. After stirring at room temperature (RT) under N_2 atmosphere for 8 h, NMP (20.2 g) was added to stir for 1 h continually. The solid content of the PAA is 12.87%, and the molecular weight (MW) is 360 000 by gel permeation chromatography. The PAA solution was diluted to 2 wt% by mixing solvent containing NMP and butyl cellosolve (BC). The ratio of NMP/BC is 60/40 by weight. The DAXIN-PI film was prepared by a spin-coating method. After the DAXIN-PI film was coated on the prepared ITO/glass substrate, the sample was prebaked at 80 °C by a heating plate for a few minutes and then baked at 230 °C under N_2 atmosphere for 30 min. The thickness of the DAXIN-PI film was estimated to be 90 nm, as measured by a scanning electron microscope (SEM). Finally, a 200-nm top aluminum electrode was deposited by e-gun evaporation through a shadow mask to form Al/DAXIN-PI/ITO ReRAM (DAXIN-PI ReRAM). The diameter of the device was 200 μm. The molecular structure of the functional DAXIN-PI is displayed in the inset in Fig. 1(b). In addition, the decomposition temperature of the DAXIN-PI was estimated to be 456 °C, as measured by a thermogravimetric analyzer.

III. Results and Discussion

Fig. 1(a) shows typical I–V characteristics of the DAXIN-PI ReRAM. Like other metal/PI-based/metal devices [5], in the initial stage, the DAXIN-PI ReRAM is in the high-resistance

Manuscript received September 16, 2012; revised September 29, 2012; accepted October 8, 2012. Date of publication November 30, 2012; date of current version December 19, 2012. This work was supported by the National Science Council of Taiwan under Contract NSC 98-2221-E-035-082-MY3. The review of this letter was arranged by Editor T. San.

S.-H. Liu is with the Ph.D. Program of Electrical and Communications Engineering, Feng Chia University, Taichung 407, Taiwan.

W.-L. Yang, M.-R. Ye, and Y.-Y. Su are with the Department of Electronic Engineering, Feng Chia University, Taichung 407, Taiwan (e-mail: wlyang@fcu.edu.tw).

C.-C. Wu is with the Graduate Institute of Biomedical Materials and Tissue Engineering, College of Oral Medicine, Taipei Medical University, Taipei 110, Taiwan.

T.-S. Chao is with the Department of Electrophysics, National Chiao Tung University, Hsinchu 330, Taiwan.

P.-Y. Wang and M.-J. Tsai are with Daxin Materials Corporation, Taichung 407, Taiwan.

Color versions of one or more of the figures in this letter are available online at http://ieeexplore.ieee.org.

Digital Object Identifier 10.1109/LED.2012.2224633

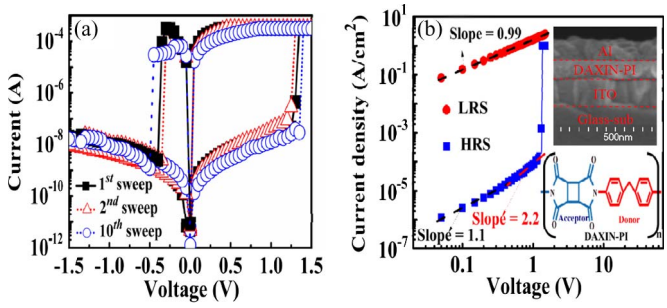

Fig. 1. (a) I–V curves of the DAXIN-PI device. The dc sweeps were repeatedly applied in light of followed voltages: 0 V $\rightarrow$ 2 V $\rightarrow$ 0 V $\rightarrow$ -1.5 V $\rightarrow$ 0 V. In the SET process, the current compliance was set to 3.14×10^{-4} A to prevent the device in hard breakdown. There is no need of an electrical forming process to induce resistance switching. (b) Linear fitting of the J–V curves in a log-log scale and the corresponding slope for each portion. The insets show the cross-sectional SEM image of the Al/DAXIN-PI/ITO/glass substrate and the molecular structure of the functional DAXIN-PI.

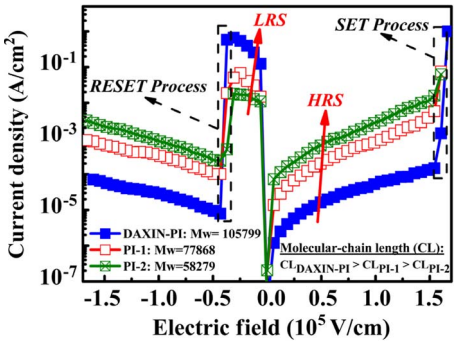

Fig. 2. J–E characteristics of PIs synthesized from MDA and CBDA with different molecular CLs. The MW of the DAXIN-PI, PI-1, and PI-2 are 105 799, 77 868, and 58 279, respectively. This represents that $\mathrm{CL_{DAXIN\text{-}PI}} > \mathrm{CL_{PI\text{-}1}} > \mathrm{CL_{PI\text{-}2}}$.

state (HRS). The DAXIN-PI ReRAM exhibits an asymmetric bipolar switching phenomenon, where V_{RESET} (ca. -0.4 V) is smaller than V_{SET} (ca. 1.3 V). In addition, it has a wide Ron/Roff ratio ($> 10^5$) at $V_{\mathrm{read}} = 0.1$ V and repeated resistance switching capability. The DAXIN-PI is based on a functional PI containing electron-donor (D) and electron-acceptor (A) moieties in a single macromolecule. In the DAXIN-PI, MDA acts as a D, whereas CBDA acts as an A. In parts of the electron-donor–acceptor-type PI system, Ling *et al.* indicated that their resistance switching is dependent to the formation and dissociation of the charge transfer (CT) complex, such as TP6F-PI and PP6F-PI [6]–[8]. The molecular orbitals of the basic unit of the DAXIN-PI are calculated by DMol3. The energy levels of the highest occupied molecular orbital (HOMO), the lowest unoccupied molecular orbital (LUMO), LUMO2, and LUMO3 are -5.63, -2.21, -1.76, and -1.18 eV, respectively. The HOMO and LUMO3 are located on D, whereas the LUMO and LUMO2 are located on A. It is found that the molecular orbital arrangement of the DAXIN-PI is similar to those of TP6F-PI and PP6F-PI. Therefore, we considered that the resistance switching of the DAXIN-PI layer could be ascribed to the formation and dissociation of the CT complex, such as TP6F-PI and PP6F-PI. As positive voltage is applied to achieve low-resistance state (LRS), the D and the A have an interaction of electron transfer to form a conductive CT complex. On the contrary, as opposite voltage is applied, the conductive CT complex is dissociated, and then, the device returns to the initial HRS. Fig. 1(b) shows $\log J$–$\log V$ characteristics of the DAXIN-PI ReRAM in the HRS and LRS. The slope of the LRS is linearly fitted to be ca. 1. This implies that the electron transport mechanism in the LRS followed ohmic conduction [7]. However, at such high current density ($\sim$1 A/cm^2) for LRS, several reports of polymer-based ReRAMs indicated that their conduction mechanism should be attributed to filament formation, which is dependent to the local electric field [9]–[11]. The cross-sectional SEM image of the DAXIN-PI thin film shown in the inset in Fig. 1(b) demonstrates that there is a low probability of inducing an obvious local electric field at SET process due to the smooth surface and the uniform DAXIN-PI thin film. In addition, I_{LRS} and I_{HRS} are strongly dependent to the device active area. With increasing the active area, I_{LRS} and I_{HRS} increase. It has been reported that I_{LRS} is unrelated to cell size for conduction-filament-based ReRAM, as cell size is larger than 90 nm [14]. Consequently, the conduction mechanism is unable to be ascribed to filament formation for DAXIN-PI ReRAM. As shown in the figure, the logarithmic plot of the J–V curve in the HRS contains two linear regions, for < 0.3 V and ≥ 0.3 V, with slopes of 1.1 and 2.2, respectively. The result illustrates that the electron conduction mechanism is dominated by the space-charge-limited conduction as the device is operated in the HRS [2]. Furthermore, the switching properties of the DAXIN-PI ReRAM are related to the thickness and the active area of the DAXIN-PI layer. With increasing the thickness of the DAXIN-PI layer, $V_{\mathrm{SET}}/V_{\mathrm{RESET}}$ and Ron/Roff increase. On the other hand, the active area closely affects the stability of Ron and Roff, that is, a small-sized DAXIN-PI ReRAM exhibits better stability than a large-sized ReRAM.

Fig. 2 shows J–E characteristics of PIs synthesized from MDA and CBDA, with different molecular chain lengths (CLs). It is shown that the PI with a long CL exhibits lower Ron and higher Roff than the PI with a short CL. With increasing the CL, the Ron/Roff ratio increases. This is because the PI with a long CL has fewer barriers between molecular chains in the LRS and fewer boundaries between molecular chains in the HRS, as compared with the PI with a short CL. When the DAXIN-PI layer is in the LRS, the electron conduction can be divided into two modes as follows: electron transport 1) in a molecular chain and 2) between molecular chains. In the process of electron transport between molecular chains, however, the barrier between molecular chains limits electron mobility. As the number of barriers between molecular chains is increased, the electron needs more energy to overcome these barriers for conducting in PI. On the other hand, when the DAXIN-PI layer is in the HRS, electron transport is dependent to deficiencies in PI, including defects within the molecular chain and boundaries between molecular chains. As deficiencies within the PI are increased, the leakage current increases. It is well known that both the number of barriers between molecular chains for LRS and the number of boundaries between molecular chains for HRS decrease with increasing the CL of the PI. This clearly indicates that the CL nearly dominates electron conduction capability in the LRS and HRS to affect switching properties. This

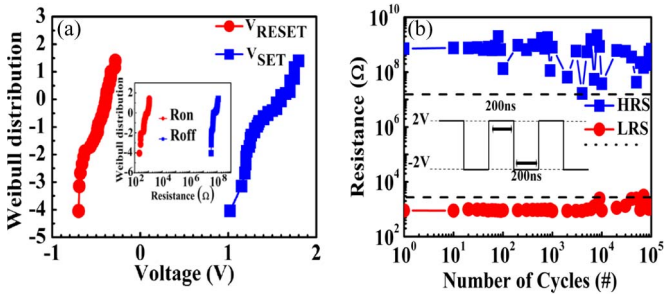

Fig. 3. (a) Weibull distribution of V_{SET} and V_{RESET} of the DAXIN-PI device. (Inset) Weibull distribution of Ron and Roff. (b) Switching endurance characteristics of the DAXIN-PI device.

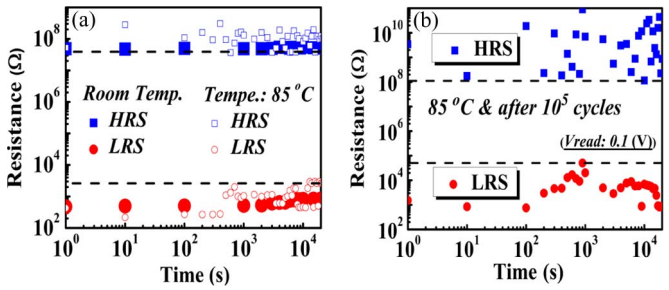

Fig. 4. (a) Resistive retention characteristics of the DAXIN-PI device at RT and 85 °C. (b) Resistive retention property at 85 °C after 10^5 SET/RESET cycles.

also explains why the DAXIN-PI layer has excellent switching properties, as compared with other electron-donor–acceptor-type PI films. This could be attributed to that the CL of the DAXIN-PI is long.

Fig. 3(a) shows statistical distribution of the switching parameters among different devices. It is shown that the narrow ranges of V_{SET} and V_{RESET} values are from 1 to 1.75 V and from -0.3 to -0.75 V, respectively. Both variations of the V_{SET} and the V_{RESET} are below 0.75 V. Furthermore, good uniformity of Ron and Roff is observed from the inset in Fig. 3(a). Both variations of the Ron and the Roff are smaller than one order. The steady switching parameters are attributed to the uniformity and stability of the sol–gel-derived DAXIN-PI thin film. Fig. 3(b) shows endurance characteristics during pulse voltage cycles. The schema of a continuous pulse voltage is displayed in the inset. The condition of the pulse voltage was from 2 to -2 V, and the period was 400 ns. As can been seen, the minimal HRS/LRS window is still maintained ca. 10^4 during 10^5 SET/RESET cycles. The unstable HRS is ascribed to the incomplete dissociation of the CT complex under RESET process.

Fig. 4(a) shows resistive retention characteristics at RT and 85 °C. As the sample was measured at RT, the HRS shows an invisible change, whereas the LRS tardily increases from 500 to 840 Ω after 10^3 s. With increasing the test temperature to 85 °C, both HRS and LRS become flaky, which are possibly ascribed to the accumulation of thermal energy, resulting in the self-formation and self-dissociation of the CT complex. Nevertheless, the minimal HRS/LRS window can be maintained ca. 10^4 at 85 °C. Fig. 4(b) displays the resistive retention at 85 °C after 10^5 SET/RESET cycles. It is found that, at 85 °C, both HRS and LRS, after 10^5 SET/RESET cycles, are flakier than those before 10^5 SET/RESET cycles, but the HRS/LRS window can be still maintained at least 10^3. We believe that the resistive retention properties of the DAXIN-PI ReRAM should be acceptable to the application of nonvolatile memory.

IV. Conclusion

A high-performance DAXIN-PI ReRAM has been fabricated, and its complete electrical properties were demonstrated. As compared with other ReRAMs, the DAXIN-PI ReRAM exhibits excellent performance in terms of needless of a forming process, large Ron/Roff ratio, fast operation speed, good uniformity of set/reset voltages, superior endurance, and acceptable retention properties. In addition, we found that the CL of PI nearly dominates the electron conduction capability in the LRS and HRS to affect switching properties for electron-donor–acceptor-type PI ReRAMs. We considered, therefore, that CL would be an important issue for PI ReRAM research in the future.

References

[1] R. Waser, R. Dittmann, G. Staikov, and K. Szot, "Redox-based resistive switching memory—Nanoionic mechanisms, prospects, and challenges," *Adv. Mater.*, vol. 21, no. 25/26, pp. 2632–2663, Jul. 2009.

[2] C. Chen, Y. C. Yang, F. Zeng, and F. Pan, "Bipolar resistive switching in Cu/AlN/Pt nonvolatile memory device," *Appl. Phys. Lett.*, vol. 97, no. 8, p. 083502, Aug. 2010.

[3] H. Zhang, L. Liu, B. Gao, Y. Qiu, X. Liu, J. Lu, R. Han, J. Kang, and B. Yu, "Gd-doping effect on performance of HfO_2 based resistive switching memory devices using implantation approach," *Appl. Phys. Lett.*, vol. 98, no. 4, p. 042105, Jan. 2011.

[4] S. G. Hahm, S. Choi, S.-H. Hong, T. J. Lee, S. Park, D. M. Kim, W.-S. Kwon, K. Kim, O. Kim, and M. Ree, "Novel rewritable, nonvolatile memory devices based on thermally and dimensionally stable polyimide thin films," *Adv. Funct. Mater.*, vol. 18, no. 20, pp. 3276–3282, Oct. 2008.

[5] N.-H. You, C.-C. Chueh, C.-L. Liu, M. Ueda, and W.-C. Chen, "Synthesis and memory device characteristics of new sulfur donor containing polyimides," *Macromolecules*, vol. 42, no. 13, pp. 4456–4463, May 2009.

[6] Q.-D. Ling, F.-C. Chang, Y. Song, C.-X. Zhu, D.-J. Liaw, D. S.-H. Chan, E.-T. Kang, and K.-G. Neoh, "Synthesis and dynamic random access memory behavior of a functional polyimide," *J. Amer. Chem. Soc.*, vol. 128, no. 27, pp. 8732–8733, Jul. 2006.

[7] Q.-D. Ling, D.-J. Liaw, E. Y.-H. Teo, C. Zhu, D. S.-H. Chan, E.-T. Kang, and K.-G. Neoh, "Polymer memories: Bistable electrical switching and device performance," *Polymer*, vol. 48, no. 18, pp. 5182–5201, Aug. 2007.

[8] Q.-D. Ling, D.-J. Liaw, C. Zhu, D. S.-H. Chan, E.-T. Kang, and K.-G. Neoh, "Polymer electronic memories: Materials, devices and mechanisms," *Progr. Polym. Sci.*, vol. 33, no. 10, pp. 917–978, Oct. 2008.

[9] B. Lei, W. L. Kwan, Y. Shao, and Y. Yang, "Statistical characterization of the memory effect in polyfluorene based non-volatile resistive memory devices," *Org. Electron.*, vol. 10, no. 6, pp. 1048–1053, Sep. 2009.

[10] W. L. Kwan, B. Lei, Y. Shao, S. V. Prikhodko, N. Bodzin, and Y. Yang, "Direct observation of localized conduction pathways in photocross-linkable polymer memory," *J. Appl. Phys.*, vol. 105, no. 12, p. 124 516, Jun. 2009.

[11] B. Chao, J.–M. Yun, S. Song, Y. Ji, D.-Y. Kim, and T. Lee, "Direct observation of Ag filamentary paths in organic resistive memory devices," *Adv. Funct. Mater.*, vol. 21, no. 20, pp. 3976–3981, Oct. 2011.

[12] B.-K. Cho, T. Yasue, H. Yoon, M.-S. Lee, I.-S. Yeo, U.-I. Chung, J.-T. Moon, and B.-I. Ryu, "Thermally robust multi-layer non-volatile polymer resistive memory," in *Proc. IEDM*, 2006, pp. 1–4.

[13] J. C. Scott and L. D. Bozano, "Nonvolatile memory elements based on organic materials," *Adv. Mater.*, vol. 19, no. 11, pp. 1452–1463, Jun. 2007.

[14] L. M. Yang, Y. L. Liu, Y. L. Wang, X. P. Tian, M. Wang, Y. Y. Lin, R. Huang, Q. T. Zou, and J. G. Wu, "Linear scaling of reset current down to 22-nm node for a novel Cu_xSi_yO RRAM," *IEEE Electron Device Lett.*, vol. 33, no. 1, pp. 89–91, Jan. 2012.